NUMERICAL MODEL STUDY ON THE EFFECT OF THE CANAL IN REDUCING TSUNAMI ENERGY

Nguyen Xuan Dao[1], Mohammad Bagus Adityawan[2], Hitoshi Tanaka[3]

ABSTRACT

A numerical model based on Reynolds Averaged Navier-Stockes (RANS) equations was used to assessed for the effects of wave-induced turbulence on the canal. The model was applied to simulate the recent Great East Japan Earthquake and Tsunami 2011, with Sendai coast as the study area. It is located in northeast part of Japan from Nanakita River towards the north up to Sendai Port which was severely damaged from the tsunami. The results revealed that the Kita-Teizan Canal which is parallel to the shoreline in Sendai coast has significant effect in reducing the tsunami energy and plays an important role in the mitigation of tsunami impacts.

1. INTRODUCTION

The recent Great East Japan earthquake with M9 on March 11th, 2011 has provided many valuable practical lessons regarding the huge consequences and potential impact of megaearthquake and megatsunamis. Sea dikes and breakwaters along Sendai coast were destroyed due to the underestimated potential of the earthquake, with a magnitude of M9 and generated tsunami off the East coast of Honshu Japan. Therefore, there is a need for scientists to understand the tsunami wave and to construct a highly resilient structure, which can mitigate the impacts of tsunamis. It is important to understand the wave interaction with breakwaters in coastal environments, in relation to the design of the hydraulic structures. Numerical studies for the solitary wave interaction with the porous breakwaters was performed by Liu and Wen (1997), while Lin and Karunarathna (2008) studied solitary wave interaction with the fully emerged rectangular porous breakwaters with different length and particle size. There have been many researches conducted to study the effect of pine trees forest, artificial and natural structures, and coastal dune in reducing tsunami energy. Coastal vegetation has been widely recognized as a natural method to reduce the energy of tsunami waves (Tanaka, 2009); However, researches on the function of a canal in terms of tsunami mitigation have not been widely carried out. Therefore, the present study aims to understand the effects of a canal in reducing the tsunami energy.

2. STUDY AREA

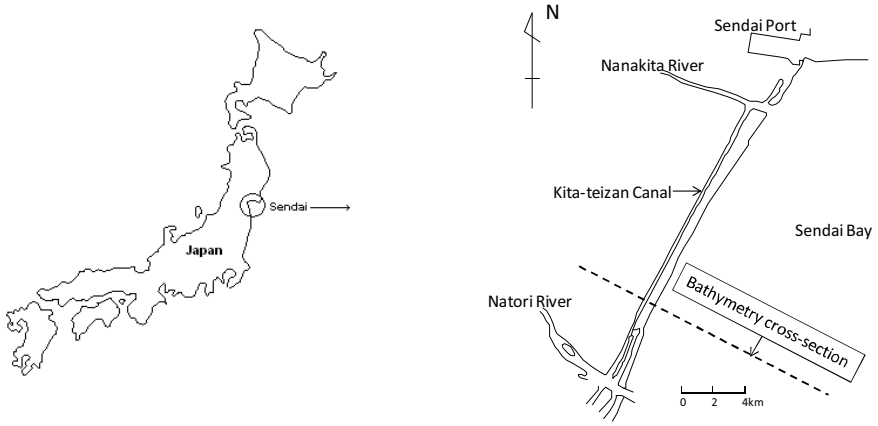

Figure 1. Map of the study area

[1] Doctoral student, Department of Civil Engineering, Tohoku University, 6-6-06 Aoba, Sendai 980-8579, Japan
[2] Post-Doctoral Researcher, Department of Civil Engineering, Tohoku University, 6-6-06 Aoba, Sendai 980-8579, Japan
[3] Professor, Department of Civil Engineering, Tohoku University, 6-6-06 Aoba, Sendai 980-8579, Japan

Sendai coast is located in the northeast part of Japan. The area was starting from the Nanakita River to the Sendai Port was severely damaged by the 2011 Tohoku earthquake and tsunami. The Kita-teizan Canal connects the Nanakita River mouth with the Natori River mouth. The length and the width of the canal are approximately 9000m and 40m. Furthermore, the canal runs parallel to the Sendai coastline at a range between 300 and 400m.

3. MODEL SETUP

This part describes the details information on the input data, initial conditions and parameters, which were used for the numerical model. The domain was set based on the surveyed bathymetry cross-section data at the location as shown in the Fig. 1. The model domain was created to represent the average bathymetric slope, distance from the shoreline to sea dikes as well as from the sea dike to the canal. The information of the sea dike and the canal such as the height and the width were provided by the official government. The computational domain is shown in Fig. 2 below.

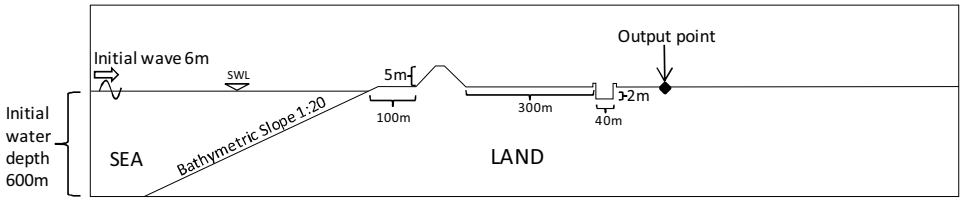

Figure 2. Computational domain setup for numerical model

A solitary wave train with a wave height of 6m and apparent period of 17 mins is sent from the left-hand boundary where the constant water depth is 600m. A beach with the slope of 1/20 is located at the other end of the domain. A sea dike with height of 5m from the ground surface is located at 100m from the shoreline. The canal with the width and the depth of 40m and 2m below the still water level is located at 240m from the backside of the sea dike. In addition, the height of the canal embankment is 0.6m.

4. NUMERICAL IMPLEMENTATION

4.1 Governing equations

In this study, a NEWFLUME model based on Reynolds Averaged Navier-Stockes (RANS) equations is applied to simulate the recent Great East Japan Earthquake and Tsunami 2011 along the coast of Sendai.

For a turbulent flow, the velocity and the pressure field can be decomposed into two parts: the mean velocity and pressure $\langle u_i \rangle$ and $\langle p_i \rangle$, and the turbulence velocity and pressure, u_i' and p'. Therefore,

$$u_i = \langle u_i \rangle + u_i' ; \quad p = \langle p \rangle + p' , \tag{1}$$

where i = 1,2,3 for a three-dimensional flow. If the fluid is assumed to be incompressible, the mean flow field is governed by the Reynolds equations as follows:

$$\frac{\partial \langle u_i \rangle}{\partial x_i} = 0 \tag{2}$$

$$\frac{\partial \langle u_i \rangle}{\partial x_t} + \langle u_j \rangle \frac{\partial \langle u_i \rangle}{\partial x_j} = -\frac{1}{\rho}\frac{\partial \langle \rho \rangle}{\partial x_i} + g_i + \frac{1}{\langle \rho \rangle}\frac{\partial \langle T_{ij} \rangle}{\partial x_j} - \frac{\partial \langle u_i' u_j' \rangle}{\partial x_j} \tag{3}$$

where ρ is the density of the fluid, g_i is the ith component of the gravitational acceleration, and $\langle T_i \rangle$ is the viscous stress tensor of the mean flow. For a Newtonian fluid, $\langle T_{ij} \rangle = 2\mu \langle \sigma_{ij} \rangle$ with μ being the molecular viscosity and the rate of strain tensor of the mean flow is

$$\langle \sigma_{ij} \rangle = \frac{1}{2}\left(\frac{\partial \langle u_i \rangle}{\partial x_j} + \frac{\partial \langle u_j \rangle}{\partial x_i}\right) \quad (4)$$

In the momentum equation (3) the influence of the turbulence fluctuations on the mean flow filed is represented by the Reynolds stress tensor, $\rho\langle u_i' u_j' \rangle$ (Lin and Liu, 1997).
An alternative to the Reynolds stress closure model is the so-called $k-\varepsilon$ in which the Reynolds stress tensor is assumed to be related to the strain rate of the mean flow through the algebraic nonlinear Reynolds stress model (Shih, Zhu and Lumley, 1996). The governing equations for $k-\varepsilon$ model are as follows:

$$\frac{\partial k}{\partial t} + \langle u_j \rangle \frac{\partial k}{\partial x_j} = \frac{\partial}{\partial x_j} + \left[\left(\frac{\nu_t}{\sigma_k} + \nu\right)\frac{\partial k}{\partial x_j}\right] + \nu_t \left(\frac{\partial \langle u_i \rangle}{\partial x_j} + \frac{\partial \langle u_j \rangle}{\partial x_i}\right)\frac{\partial \langle u_i \rangle}{\partial x_j} - \varepsilon \quad (5)$$

$$\frac{\partial \varepsilon}{\partial t} + \langle u_j \rangle \frac{\partial \varepsilon}{\partial x_j} = \frac{\partial}{\partial x_j} + \left[\left(\frac{\nu_t}{\sigma_\varepsilon} + \nu\right)\frac{\partial \varepsilon}{\partial x_j}\right] + C_{1\varepsilon}\frac{\varepsilon}{k}\nu_t \left(\frac{\partial \langle u_i \rangle}{\partial x_j} + \frac{\partial \langle u_j \rangle}{\partial x_i}\right)\frac{\partial \langle u_i \rangle}{\partial x_j} - C_{2\varepsilon}\frac{\varepsilon^2}{k} \quad (6)$$

in which, σ_k, σ_ε, $C_{1\varepsilon}$ and $C_{2\varepsilon}$ are empirical coefficients. The recommended values (Rodi, 1980) for these coefficients are as follows:

$$C_{1\varepsilon} = 1.44,\ C_{2\varepsilon} = 1.92,\ \sigma_k = 1.0,\ \sigma_\varepsilon = 1.3 \quad (7)$$

4.2 Boundary and initial conditions

Appropriate boundary conditions need to be specified for the model. For a rigid boundary conditions, the values of k and ε are expressed as functions of distance from the boundary and the mean tangential velocity outside of the viscous sublayer. For the free surface boundary condition, the zero-gradient are imposed for both k and ε .
The initial condition for the mean flow is treated as still water with no wave or current motion (Lin and Liu, 2000).

The volume of fluid (VOF) is used to track the free-surface locations through the wave breaking process. The method was originally developed by Hirt and Nichols (1981) and has been modified by Kothe et al. (1991)

An initial of off-shore wave boundary condition (x = 0) was generated by using solitary wave equation in constant depth is given as follows:

$$\zeta(t) = a\,sech^2\left[\left(\frac{3a}{4d^3}^{1/2}\right)(-ct)\right] \quad (8)$$

in which, a is the wave height, d is the constant depth, and $c = [g(d+a)]^{1/2}$ is the wave celerity at constant water depth.

5. RESULTS AND DISCUSSIONS

The model was set up to simulate tsunami propagation and run-up in Sendai coast for two cases with a canal and without a canal to evaluate the effect of canal in reducing tsunami. In addition, an output point which can be seen in Fig. 2 is given to estimate the effect of canal into the tsunami propagation.

5.1 Effect of canal to flux discharge, tsunami depth-averaged velocity

Table 1 shows the tsunami depth-averaged velocity at the point after the canal is 11.67 m/s, the tsunami inundation depth is 4.89 m and the maximum discharge flux become 57.09 m^2/s after approximately 14 minutes tsunami travel from the open boundary. Whereas, in the case without canal, the tsunami depth-averaged velocity is 13.43 m/s, the tsunami inundation depth becomes 4.82 m, and the maximum flux

discharge becomes 64.74 m^2/s. It can be noted here that the flux discharge reduction was 7.65 m^2/s due to the effect of the canal in this case.

Table 1: Flow discharge, depth-averaged velocity and inundation depth in two cases

	Without canal	With canal	Difference
Discharge (m^2/s)	64.74	57.09	7.65
Depth-averaged velocity (m/s)	13.43	11.67	1.76
Inundation depth (m)	4.82	4.89	0.07

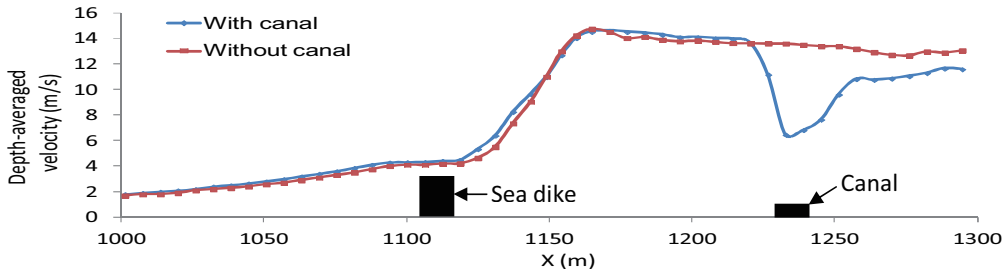

Figure 3: Tsunami depth-averaged velocity profile in two cases (with and without canal)

Fig. 3 shows the tsunami depth-averaged velocity profile from offshore into land. It can be seen that the depth-averaged velocity in the case with canal was suddenly decreased at the canal comparison with the case without canal.

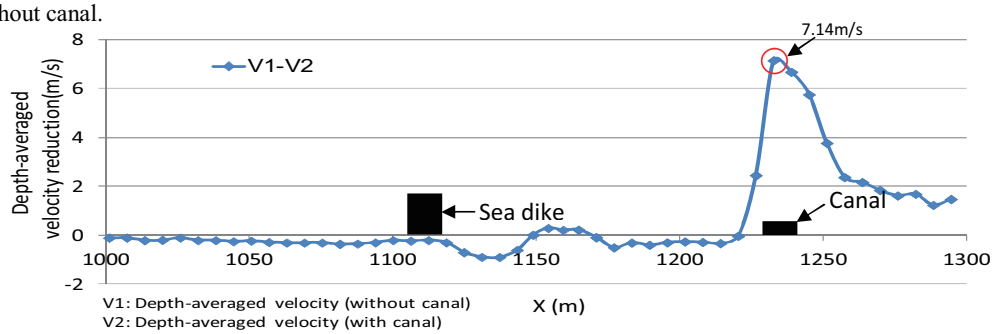

Figure 4. Tsunami depth-averaged velocity reduction due to the effect of the canal

To estimate maximum depth-averaged velocity reduction effects of the canal, with and without canal tsunami depth-averaged velocity is subtracted. Fig. 4 shows the differences of maximum depth-averaged velocity reduction. It can be seen that due to the effect of the canal, the maximum depth-averaged velocity reduced 7.14 m/s. This phenomenon can be explained by the effect of the canal, it takes time for tsunami to fill up water into the canal before running up further inland. Also, because of the tsunami energy dissipation into the canal, therefore, the tsunami depth-averaged velocity was reduced resulting delayed tsunami arrival time in the case with canal.

It can be clearly seen from Fig. 5 that at the snapshot 84 minutes, in the case with canal, the tsunami still had not reached the end of the domain whereas in the case without canal the tsunami had already passed it. Moreover, according to the snapshots 84 and 98 minutes, in the case with canal, the tsunami depth-averaged velocities were significantly reduced comparison with the case without canal.

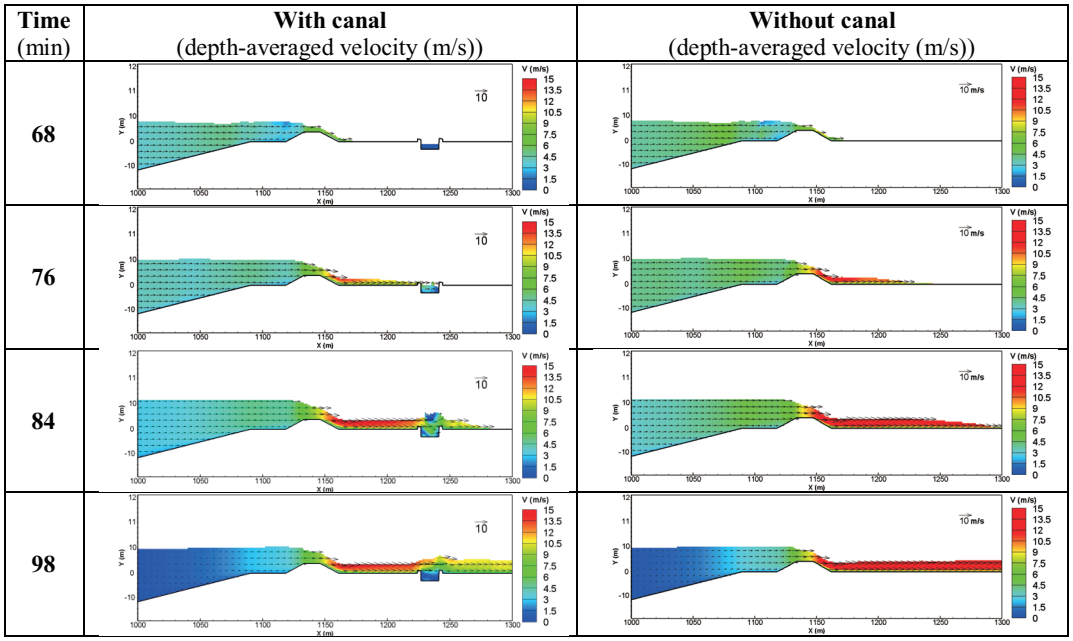

Figure 5: Tsunami depth-averaged velocity in two cases (with and without canal)

5.2 Effect of the canal to wave energy dissipation

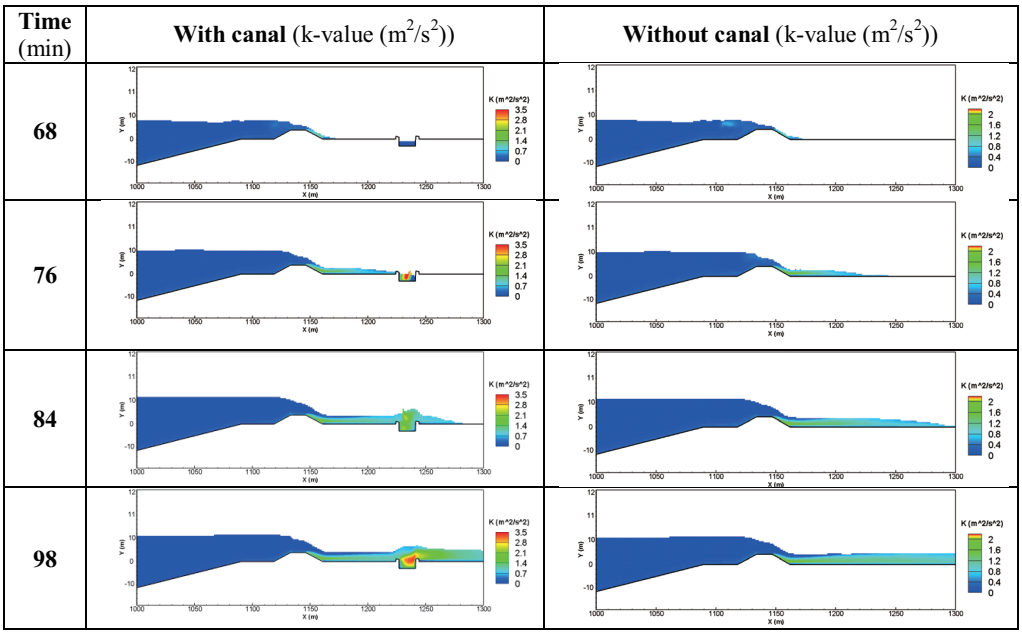

Figure 6: Turbulence kinetic energy value in two cases (with and without canal)

Fig. 6 shows that the maximum turbulence kinetic energy induced by surface layer was approximately 3.5 m^2/s^2 located inside the canal. In addition, at the snapshot after 76, 84 and 98 minutes, it can be seen that the tsunami kinetic energy production was increased at the canal and much higher than the kinetic energy in the

case without canal. The increase of kinetic energy production at the canal will cause the tsunami wave energy dissipation and resulting reducing its energy. Therefore, the canal was effective in reducing tsunami energy.

6. CONCLUSIONS

The model has been successfully applied to simulate tsunami run-up as well as the effects of canal in reducing tsunami energy. Moreover, the results showed that the effect of Kita-Teizan canal in reducing tsunami energy was significant. Therefore, in terms of multiple defenses, the canal should be taken into account. Especially, in the largest tsunami, the canal embankment should be increased in both dimension height and width in order to be able to withstand and be more effective in reducing tsunami energy in the future.

ACKNOWLEGEMENTS

The authors would like to express their grateful thanks to Professor Pengzhi Lin of Sichuan University for providing the latest version of NEWFLUME. The appreciation is extended to the Sendai Office, Miyagi Prefecture for their kind supply of the valuable field data. This research could not be conducted without financial supports from the Grant-in-Aid for Specific Research Project, International Research Institute of Disaster Science, Tohoku University. The Grant-in-Aid for Scientific Research from JSPS (No. 22360193, No. 2301367).

REFERENCES

Hirt, C.W. and Nichols, B. D. (1981). Volume of fluid (VOF) method for dynamics of free boundaries. *J. Comput. Phys*. 39, 201–225.

Kothe, D. B., Mjolsness, R. C. and Torrey, M. D. (1991). RIPPLE: A computer program for incom- pressible flows with free surfaces. Los Alamos National Laboratory, LA-12007-MS.

Lin, P., Karunarathna, SASA., Numerical study of solitary wave interation with porous breakwaters. *J Waterway Port Coastal Ocean Engineering* (2007). 133, 352-63.

Lin, P., and Liu , P. L.-F., (1998). "A numerical study of breaking waves in the surf zone." *Journal of Fluid Mechanics* 359, 239–264.

Liu, P. L.-F. and Wen, J., (1997). "Nonlinear diffusive surface waves in porous media". *Journal of fluid Mechanics* 347, 119-139.

Rodi, W. (1980). *Turbulence Models and Their Application in Hydraulics – A State-of-the-Art Review*. IAHR Publication.

Shih, T.-H., Zhu, J. and Lumley, J. L., (1996). Calculation of wall-bounded complex flows and free shear flows. *Intl J. Numer. Meth. Fluids 23, 1133-1144.*

Suntoyo, Tanaka, H. (2009). Numerical modeling of boundary layer flows for a solitary wave. *Journal of Hydro-environment Research*, *3*(3), 129–137. doi:10.1016/j.jher.2009.05.004

Tanaka, N. (2009). "Vegetation bioshields for tsunami mitigation: review of effectiveness, limitations, construction, and sustainable management." *Landscape and Ecological Engineering* 5(1), 71–79.

Tanaka, H., Tinh, N. X., Umeda, M., Hirao, R., Pradjoko, E., Mano, A., and Udo, K., (2012). Coastal and Estuarine Morphology Changes Induced By the 2011 Great East Japan Earthquake Tsunami. *Coastal Engineering Journal*, *54*(01), 1250010 (25 pages). doi:10.1142/S0578563412500106

Thuy, B. N, Tanimoto, K., Tanaka, N., Harada, K., and Iimura, K. (2009). "Effect of open gap in coastal forest on tsunami run-up—investigations by experiment and numerical simulation." *Ocean Engineering* 36(15-16):1258–1269.